17th World Conference on Earthquake Engineering, 17WCEE
Sendai, Japan - September 13th to 18th 2020

AN UPGRADED PARAMETER MODEL FOR ROCKING-WALL MOMENT FRAME STRUCTURES

Y. Chen[(1)], DS Yao[(2)], QQ. Li[(3)]

[(1)] *Chair of Civil Engineering Department, Research Center of Industrialization, Construction Technology, Ningbo University of Technology, Ningbo, China, ychen@nbut.edu.cn*
[(2)] *State Key Laboratory of Disaster Reduction in Civil Engineering, Tongji University, Shanghai, China, 2327575656@qq.com*
[(3)] *Enrolled Graduate Student, Research Center of Industrialization, Construction Technology, Ningbo University of Technology, Ningbo, China, qqli@nbut.edu.cn*

Abstract

Rocking-wall moment frames (RWMF) are unique, lateral resisting structures which consist of rocking-walls and moment frames. Prior studies have demonstrated that RWMF can prevent soft-story failure, reduce drift concentration and provide suitable supports for energy-dissipating devices compared with traditional moment frames. Normally, a distributed parameter model (DPM) is used to describe the performance of RWMF, which consists of a flexural beam and a shear beam connected by infinite rigid links. The flexural beam and the shear beam represent the wall and the frame, respectively. However, to simplify the frame into a shear beam is not appropriate. Besides, the infinite rigid links cannot manifest the interaction between the frame and the wall properly. In this paper, an upgraded parameter model named continuous discrete model (CDM) is proposed to simulate RWMF. Specifically, 1) Instead of a shear beam, a lumped mass model is employed to simulate the frame; and 2) The rocking-wall and the frame are connected only at several positions, such as floor levels. The results via CDM are compared with those by DPM. In addition, a parameter analysis was carried out based on CDM. The results indicate that the upgraded parameter model can reflect the performance of RWMF effectively and more realistically compared with DPM.

Keywords: Rocking wall; Moment frame; parameter model; Drift concentration factor; Parameter analysis

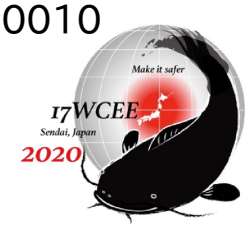

1. Introduction

Damage due to soft-story mechanisms is dangerous for a frame structure in earthquakes [1]. A rocking-wall moment frame structure (RWMF) was proposed by Alavi et al. to reduce the concentration of frame deformation at a certain level, largely at the ground level [2]. RWMF is a special type of structure, in which, the base of structure is connected to the foundation using a pin connection. If the pin-supported rocking wall is well-designed, it will have adequate rigidity to control the deformation pattern of the moment frame [2]. It has been proved RWMF can effectively reduce the damage caused by earthquakes [3].

The exploration of the behavior of RWMF is increasingly popular due to its excellent performance. Traditionally, a double beam model (DBM, see Fig.1(a)), which contains a flexural beam and a shear beam, was first proposed by Khan et al. [4] to study the behavior of shear-wall frame structures[5]. Based on DBM, an improved parameter model, DPM (see Fig.1(b)) was developed and widely applied to investigate the performance of RWMF. The major difference between DBM and DPM is the connection of the wall to the base. Specifically, different from DBM, the flexural beam of DPM, which represents the wall, has a hinged connection to the base. Pan et al. investigated the interior forces and strength demands of the pin-supported rocking wall through DPM utilizing static analysis [6]. On this foundation, Wu et al. studied the effects of relative stiffness on modal shapes, effective modal mass ratios, and the influence of higher mode effects on the displacement and interior forces of RWMF [7]. Wiebe et al. added a rotational spring to the base of the wall and the higher-mode effect was considered [8]. Feng et al. illustrated the strength demand of the wall and the buckling restrained braces, which were modeled by a rotational spring when the frame enters the inelastic stage of behavior [9].

In both DBM and DPM, the two beams are connected by infinite rigid links, which transmit horizontal forces between them [6, 10]. Hence, the deformation of the two beams is identical over the entire height of the structure. However, due to this assumption, the curves of the internal forces obtained using DPM is smooth and without any abrupt changes. This phenomenon is inconsistent with the reality.

To overcome these disadvantages, in this research, an improved parameter model named continuous discrete model (CDM) is developed based on the existing research. Specifically, 1) Instead of a shear beam, a lumped mass model is employed to simulate the frame under seismic loads [11]; and 2) The rocking wall and the moment frame are connected only at several positions, such as floor levels. The boundary conditions and the special solutions of CDM under different load distributions are presented. Moreover, the effectiveness of the improved parameter model is verified using OpenSees. Finally, the results from CDM are compared with those from DPM and then parameter analysis is executed via CDM.

2. Continuous Discrete Model

As is shown in Fig. 1(c), a multistory building is modeled as the combination of two components connected with rigid links at the location of floors. The hinged flexural beam and the lumped mass model simulate the wall and the frame, respectively. The total height of the model is denoted as H. It is assumed that the height and the stiffness of each floor are equal and denoted as h and k, respectively. The number of stories is written as n.

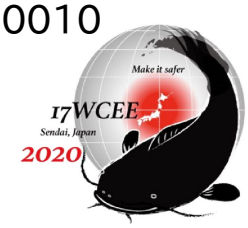

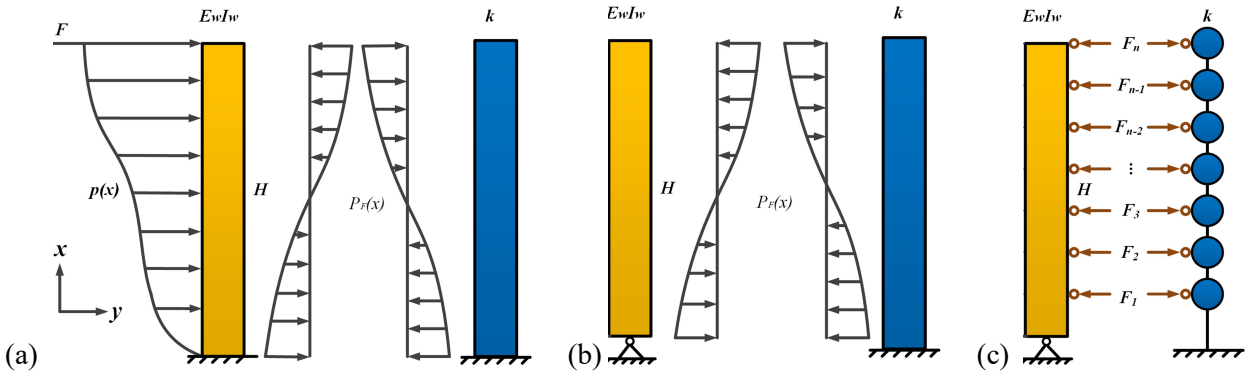

Fig. 1 – Parameter models: (a) Double Beam Model (DBM);
(b) Distributed Parameter Model (DPM); (c) Continuous Discrete Model (CDM)

For these three types of parameter models, according to the basic relationship between the displacement and inner forces, an identical differential equation can be expressed as

$$E_w I_w \frac{d^4 y}{dx^4} = p(x) \tag{1}$$

where E_wI_w is the bending stiffness of the wall, $y(x)$ is the lateral displacement of the wall at the height of x and $p(x)$ is the distribution of the external load. For convenience, a dimensionless parameter is defined as

$$\xi = \frac{x}{H} \tag{2}$$

Where ξ means the relative height of the structure.

Using this dimensionless parameter, the differential equation, Eq.(1), can be rewritten as

$$\frac{d^4 y}{d\xi^4} = \frac{p(\xi) H^4}{E_w I_w} \tag{3}$$

The general solution for Eq. (3) can be expressed as
For DBM, DPM [6]:

$$y = A + B\xi + C\sinh\lambda\xi + D\cosh\lambda\xi + y_p \tag{4}$$

and for CDM:

$$y = A\xi^3 + B\xi^2 + C\xi + D + y_p \tag{5}$$

Note that in Eqs. (4) and (5), y_p is a particular solution.
If the displacement expression $y(x)$ is given, the displacement at the floor level can also be identified. Therefore, the shear force of the wall can be acquired through the following equations:

$$\theta = \frac{dy}{dx} = \frac{1}{H}\frac{dy}{d\xi} \tag{6}$$

$$V_w = -E_w I_w \frac{d^2\theta}{dx^2} = -\frac{E_w I_w}{H^3}\frac{d^3 y}{d\xi^3} \tag{7}$$

The moment of the wall is also given by

$$M_w = E_w I_w \frac{d\theta}{dx} = \frac{E_w I_w}{H^2}\frac{d^2 y}{d\xi^2} \tag{8}$$

Different from DBM and DPM, the flexural beam and the lumped mass model have the same deformation only at the heights of the rigid links which are set at the floor levels. Meantime, the shear force of the *j*th floor of the frame can be obtained as

$$V_{fj} = k(y_j - y_{(j-1)}) \tag{9}$$

where y_i is the displacement at the *j*th floor level. Note that y_0=0 is the displacement of the bottom of the first floor. In addition, CDM is also capable of giving the forces in the rigid links, which can benefit the design of these links. The force at the *i*th floor is denoted as F_i and can be given into

(1) When $0 \leq i < n$,

$$F_i = V_{(i+1)} - V_i \tag{10}$$

(2) When $i=n$,

$$F_i = V_i \tag{11}$$

Three specific load profiles [6] (namely, a uniformly distributed load, an inverted triangular distributed load, and a concentrated load at the top) are considered and the boundary conditions of DBM and DPM can be defined as
For DBM:

$$\begin{cases} M_W = 0 \ , \xi = 1 \\ y = 0 \quad , \xi = 0 \\ \theta = 0 \quad , \xi = 0 \\ V = \begin{cases} F, \xi = 1 & for\ the\ concentrated\ load\ at\ the\ top \\ 0, \xi = 1 & for\ the\ uniformly\ or\ inverted\ distributed\ load \end{cases} \end{cases} \tag{12}$$

and for DPM:

$$\begin{cases} M_W = 0 \ , \xi = 0, 1 \\ y = 0 \quad , \xi = 0 \\ V = \begin{cases} F, \xi = 1 & for\ the\ concentrated\ load\ at\ the\ top \\ 0, \xi = 1 & for\ the\ uniformly\ or\ inverted\ distributed\ load \end{cases} \end{cases} \tag{13}$$

where F is the value of the concentrated load at the top.

Eqs. (12) and (13) indicate that the constraints contain both the boundary conditions and the deformation compatibility conditions, respectively. Furthermore, it is obvious that the constraints' conditions for CDM vary from DBM and DPM. Accordingly, the different solutions will be obtained for the differential equation of CDM compared with DBM and DPM. In addition, these constraints change with the total number of the stories of the frame as well as the unknown coefficients of the differential equation here written as A_1, B_1, C_1, D_1 to A_n, B_n, C_n, D_n. The mathematical expression of the constraints applicable for the frame with any number of stories under the preceding three specific load profiles can be derived via Matlab.

3. Model Verification

DPM assumes the horizontal forces can be transferred at any location on the interface between the frame and the wall. In contrast, CDM's assumption is that the horizontal force can only be transferred at floor levels through the rigid links. As mentioned in section 2, these horizontal forces acting in the rigid links can also be acquired. To confirm the effectiveness of CDM and investigate the difference between DPM and CDM, the analytical results via CDM are compared with those via DPM and the OpenSees model employing a practical building. This building had been completed in the Sichuan province of China [6].

3.1 Case Study

Fig. 2 shows a two-dimensional five-story RWMF model in OpenSees. The bending stiffness of the frame beams is assumed to be infinite. Note that in DPM, K corresponds to the shear force when a unit inter-story drift is applied. Accordingly, in CDM, k corresponds to the shear force when a unit inter-story displacement is applied and can be expressed as

$$k = \frac{GA}{h} \tag{14}$$

where h is the story height, G is the shear modulus and A is the cross-sectional area[12]. In this case, $K = 1.86 \times 10^6 \mathrm{kN}$ and $k = 6.2 \times 10^5 \mathrm{kN/m}$. Two sizes of walls are considered. The cross-sections of the walls are 2.0 × 0.6 m and 4.0 × 0.6m, respectively.

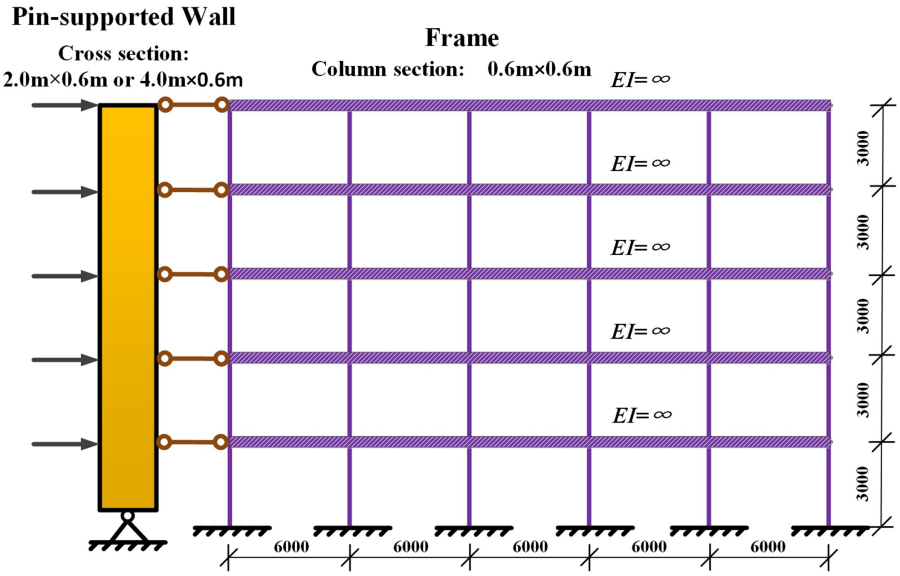

Fig.2 – OpenSees model of the five-story RWMF

In the OpenSees model, both beams and columns of the frame are modeled by ElasticBeamColumn elements. The wall is modeled by NonlinearBeamColumns elements and is hinged at the bottom [13]. The structure is loaded with concentrated loads at the floor level. Two forms of concentrated loads are considered: The Concentrated Loads converted from the Uniformly Distributed load (CLUD) and the inverted Triangular Distributed load (CLTD), respectively.
For convenience, a dimensionless parameter is defined as

$$\lambda = H^3 \frac{k}{E_w I_w} \tag{15}$$

where λ means the relative stiffness of the wall and the frame. A small λ indicates a relatively stiff wall, while a large λ indicates a relatively flexible wall. The Drift Concentration Factor (DCF), recommended by Macrae et al.[14], is utilized to assess the uniformity of the inter-drift ratio and is defined as

$$\mathrm{DCF} = \frac{\max_i \frac{d_i}{h_i}}{\Delta / \sum_i h_i} \tag{16}$$

where the interstory displacement, the story height and the roof displacement are symbolized by d_i, h_i and Δ, respectively. A small DCF corresponds to a good uniformity and vice versa. Ideally, when DCF is equal to 1, inter-drift ratios in all stories are identical.

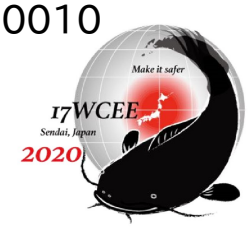

3.2 Definition of concentrated loads

For the convenience of comparison of the two parameter models and considering the overturning effect of the concentrated load at the top story, this section uses the same assumption with Pan et al.[6]which add a concentrated load at the top of DPM and CDM. The concentrated loads in the OpenSees model at each story are denoted as F_{ci}. Particularly, the load at the top story is denoted as F_{ctop}. The concentrated load at the top story in DPM is taken to be $F_{ctop}/2$ to maintain an identical base shear for the OpenSees model and other two parameter models. The distributed load in the parameter models satisfies

$$\sum_{i=1}^{n} F_{ci} - \frac{F_{\text{ctop}}}{2} = \int_0^1 p\,(\xi)\,d\xi \tag{17}$$

In the case for CLUD, $F_{c1} - F_{c2} - \cdots F_{ci} \cdots - F_{ctop}$ for the OpenSees model and $p(\xi) = q$ for DPM and CDM. And in the case for CLTD, $F_{ci} = \frac{i}{n} F_{ctop}$ for the OpenSees model and $p(\xi) = q\xi$ for DPM and CDM.

In this research, four cases are considered for the verification:

(a) wall depth=2m, λ=174.4, CLUD, DCF=1.51;
(b) wall depth=2m, λ=174.4, CLTD, DCF=1.31;
(c) wall depth=4m, λ=21.8, CLUD, DCF=1.19;
(d) wall depth=4m, λ=21.8, CLTD, DCF=1.13.

In cases (a) and (c), the concentrated load is 3.33×10^2 kN for all stories. Accordingly, in cases (b) and (d), the concentrated load at the top is 3.00×10^2 kN.

3.3. Results' analysis

The story displacement, the bending moment, and the shear force of the wall obtained through CDM, DPM and OpenSees are compared in Fig.3, respectively. The blue lines with diamonds represent the results via CDM while the pink asterisks illustrate those using the OpenSees model. The solutions for CDM are obtained via Matlab. The parameter models provide the continuous solutions at various heights, whereas the OpenSees model furnishes the discrete values of each story.

From Fig.3, we can see that the story displacement, the bending moment, and the shear force using CDM are very close to those through the OpenSees model. In all cases, the top displacement and the bending moment attained by CDM are larger than those by the OpenSees model. This may be due to the effect of the shape of the columns' cross sections were neglected so that the stiffness of the frame has been underestimated[15]. To verify the accuracy of CDM, the top displacement, the maximum moment and the shear force by dint of CDM and the OpenSees model are compared in Table 1. From Table 1, the errors are less than 11% for all variables.

As is shown in Fig. 4, the forces in the rigid links obtained through CDM are similar to those by OpenSees model. However, the force acting in the rigid link of the top floor is much larger than those acting in other rigid links of other floors. Most of the time, the OpenSees model gives slightly greater values than CDM for the forces in the rigid links and the errors are all less than 12%.

In general, CDM and the OpenSees models agree well in all four cases. By this comparison, it can be proved that CDM is accurate and effective.

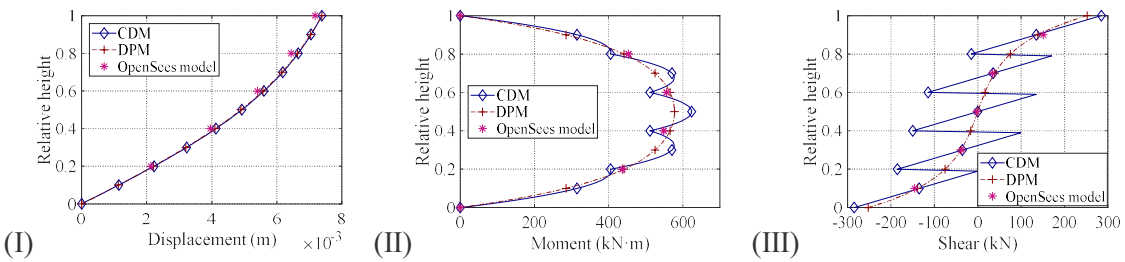

(a) wall depth=2m, λ=174.4, CLUD, DCF=1.51

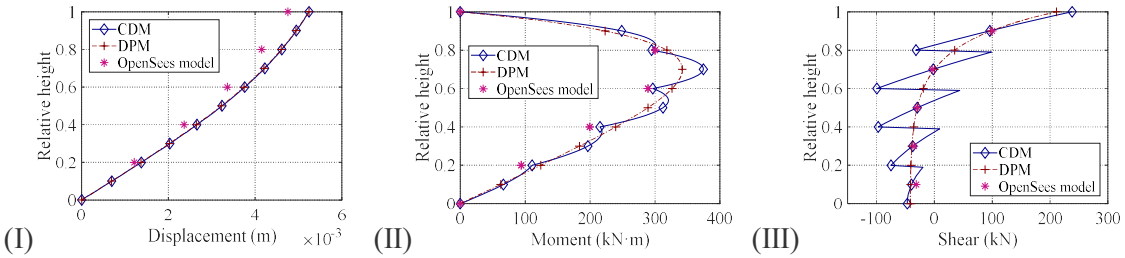

(b) wall depth=2m, λ=174.4, CLTD, DCF=1.31

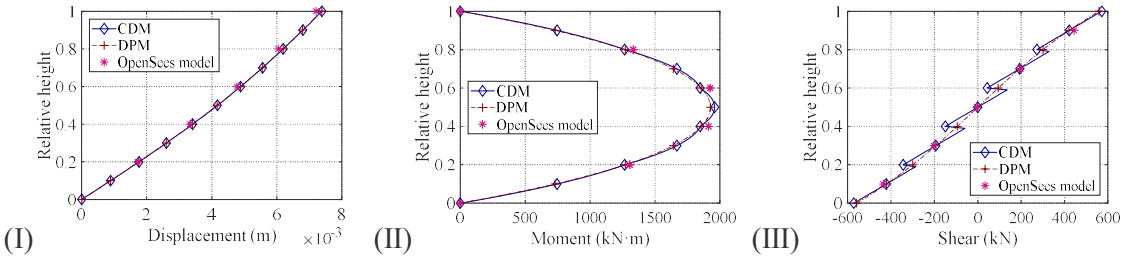

(c) wall depth=4m, λ=21.8, CLUD, DCF=1.19

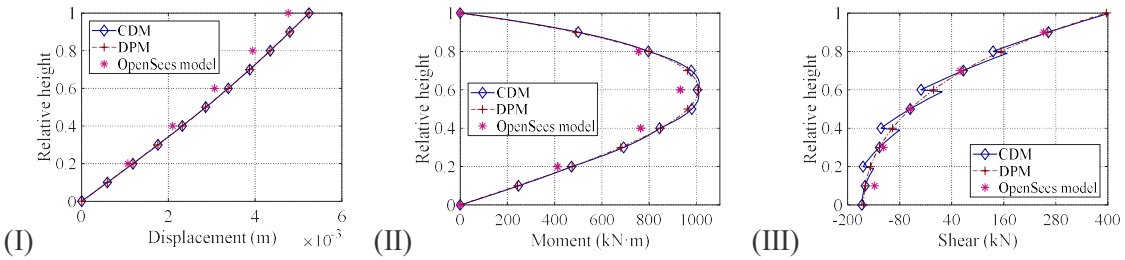

(d) wall depth=4m, λ=21.8, CLTD, DCF=1.13

Fig.3 – Comparisons of the displacement, the bending moment, and the shear force of the wall in DPM, CDM and the OpenSees model

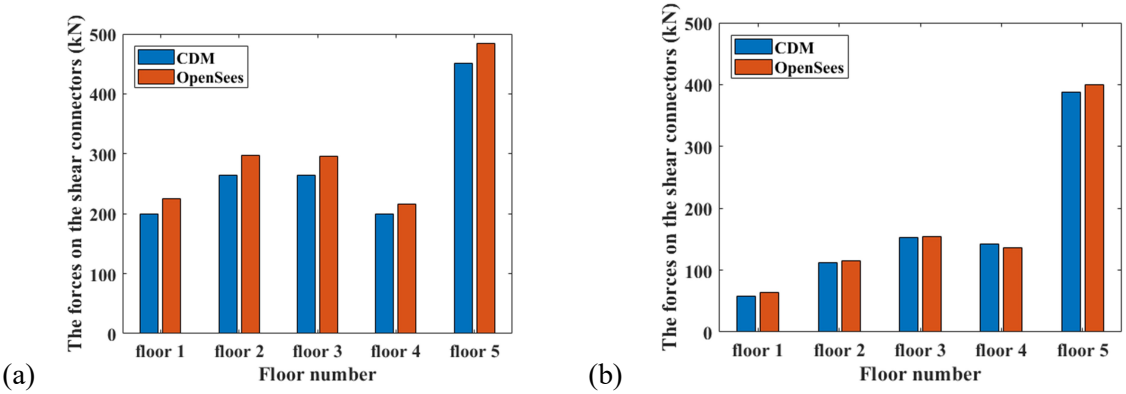

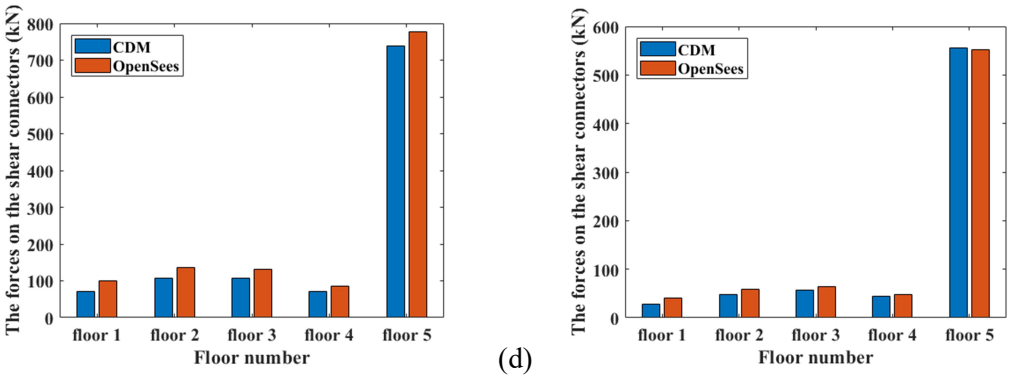

Fig.4 – Comparisons of forces in the rigid links in DPM, CDM and the OpenSees model: (a) wall depth=2m, λ=174.4, CLUD, DCF=1.51; (b) wall depth=2m, λ=174.4, CLTD, DCF=1.31; (c) wall depth=4m, λ=21.8, CLUD, DCF=1.19; (d) wall depth=4m, λ=21.8, CLTD, DCF=1.13

Table 1 – Comparison of the top displacement, maximum moment, and maximum shear obtained using CDM and the OpenSees model

Variable	Case	CDM	OpenSees model	Error
Top displacement (mm)	a	7.4	7.2	2.9%
	b	5.2	4.8	10.3%
	c	7.4	7.2	2.5%
	d	5.2	4.8	10.1%
Maximum moment (kN·m)	a	511.2	555.8	8.0%
	b	296.5	300.2	1.2%
	c	1846.9	1924.7	4.0%
	d	1004.2	932.6	7.7%
Maximum shear (kN)	a	135.0	151.2	10.7%
	b	95.8	100.1	4.3%
	c	422.0	444.5	5.1%
	d	262.8	251.8	4.4%

3.4. Comparison between DPM and CDM

The differences between DPM and CDM for this case are also shown in Fig.3. The red dot dash lines with plus signs symbolizes the results from DPM. Compared with DPM, CDM gives very similar displacement (see Fig.3(I) of each subgraph) while the internal forces acting within the wall are more realistic (see Fig.3(II) and (III) of each subgraph). The maximum bending moment, the shear force and their differences of each case via DPM and CDM are shown in Table 2. As is shown in Fig.3 and Table 2, the distribution curves of the internal forces utilizing CDM changes abruptly than those through DPM. In addition, the maximum bending moments and the maximum shear forces obtained using CDM are always larger than those via DPM. From Table 2, The maximum shear forces via CDM in case a and b are 12.9% larger than those obtained through DPM. Accordingly, the maximum bending moments via CDM in case a and b are 8.0% and 9.5% larger than those using DPM, respectively. According to the above analysis, we can see that DPM underestimate the internal forces of RWMF compared with CDM. Consequently, there is no doubt that CDM

can reflect the performance of RWMF effectively and more realistically than DPM. Besides, CDM can provide the forces in the rigid links which can benefit the design of these links as well.

Table 2 – Comparisons of the maximum moments and the shear forces using CDM and DPM

Variable	Case	CDM	DPM	Error
Maximum bending moment (kN·m)	a	623.6	577.4	8.0%
	b	374.4	341.9	9.5%
	c	1959.3	1926.0	1.7%
	d	1011.8	1008.5	0.3%
Maximum shear force (kN)	a	284.9	252.4	12.9%
	b	238.3	211.0	12.9%
	c	571.9	559.4	2.2%
	d	405.3	396.8	2.2%

4. Parametric analysis of CDM

4.1 Effect of the wall stiffness on the displacement distribution

Fig. 5 shows the effects of λ on the drift concentration factors obtained using CDM and DPM for the five story structure under the uniformly distributed load and the inverted triangular distributed load, respectively. Compared with DPM, it is apparent that CDM provides larger values of DCF according to Fig. 5. This phenomenon is due to the difference of their basic assumptions. Specifically, DPM assumes that the two beams are connected by infinite rigid links. Too many constraints are exerted on RWMF owing to this assumption so that the capabilities of the walls to control the deformation of the frames are overestimated.

Besides, as is shown in Fig. 5, DCF changes most severely when λ is less than 155. By contrast, when λ varies from 155 to 3500, the DCFs only increase 13.77% and 6.36% in CDM under the uniformly distributed and the inverted triangular distributed load, respectively. This observation demonstrates that FWPS should be designed with λ<155 in order to effectively control the deformation of the structure. Moreover, it is clear that the pattens of horizontal distributed loads have less effect on the rate of change of DCF while λ plays a dominant role to it according to Fig. 5.

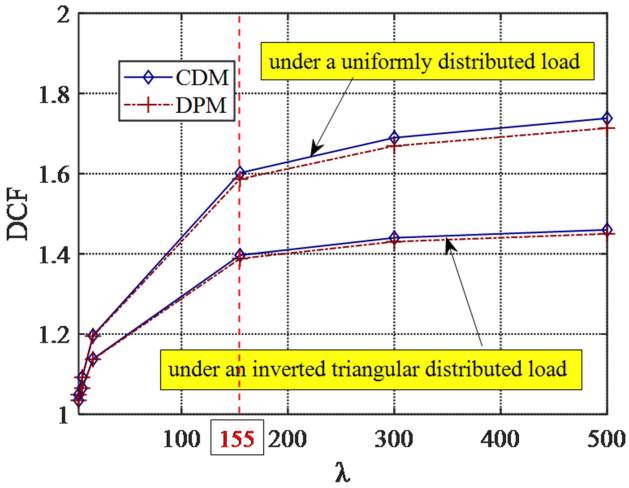

Fig.5 – Comparisons of DCF for DPM and CDM (λ = 10 to 500)

4.2 Effect of the wall stiffness on the forces acting in the rigid links

As is shown in Fig.6, when λ varies from 10 to 155, the forces acting in the rigid link of the top floor dramatically decrease 54.27% under the uniformly distributed load and 44.96% under the inverted triangular distributed load while those acting in the rigid links of other floors all gradually increase. By contrast, when λ >155, the changes of the forces reduce significantly.

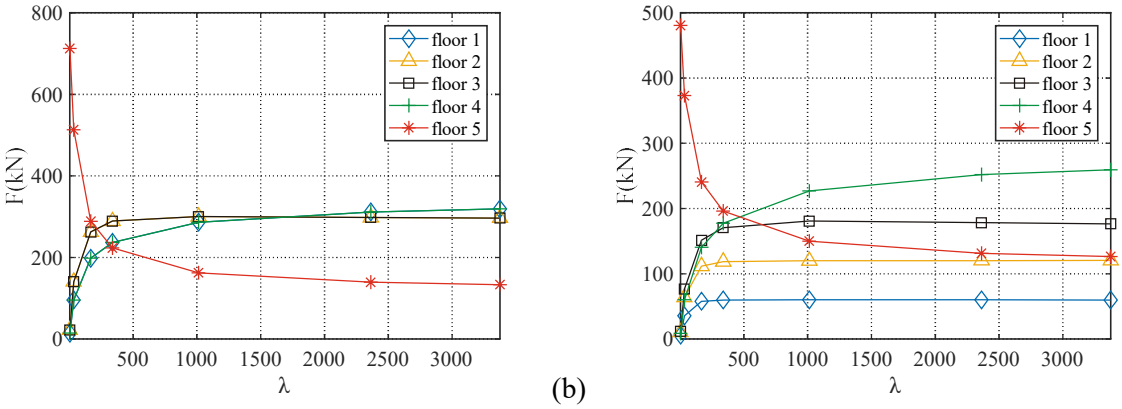

Fig.6 – Influence of λ on the forces acting in the rigid links: (a) uniformly distributed load; (b) inverted triangular distributed load

According to Fig.5, when DCF is effectively controlled, λ should not be too large. In this case, in the light of Fig.6, the force in the rigid link of the top floor will be much larger than those in other stories when $\lambda < 155$. As a result of this, the rigid links of the top floor must be designed carefully in order to avoid the damage owing to the stress concentration.

5. Conclusions

In this paper, an upgraded parameter model named continuous discrete model is proposed, verified and then applied to investigate the performance of Rocking-Wall Moment Frame Structures. Meanwhile, the characteristics of the Continuous Discrete Model are compared with the Distributed Parameter Model. The following conclusions can be drawn:

(1) By comparing the Continuous Discrete Model, the Distributed Parameter Model and the OpenSees model, it is clear that the Continuous Discrete Model can reflect the performance of Rocking-Wall Moment Frame Structures effectively and accurately. In addition, it can be confirmed that the Continuous Discrete Model can provide more reliable and conservative values for the internal forces than the Distributed Parameter Model. The Continuous Discrete Model can be employed to the preliminary design of Rocking-Wall Moment Frame Structures.

(2) The Drift Concentration Factor can be utilized to evaluate the uniformity of Rocking-Wall Moment Frame Structures. If Drift Concentration Factors are effectively controlled, namely the interstory deformations of all floors are similar, the relative stiffness of the pin-supported rocking wall and the moment frame λ should be less than 155.

(3) When λ is less than 155, the force acting in the rigid link of the top floor will be much larger than other links. Hence, the links of the top floor should be carefully designed to avoid the damage owing to the stress concentration.

(4) The pattens of horizontal distributed loads have less effect on the rate of change of DCF while λ plays a dominant role to it.

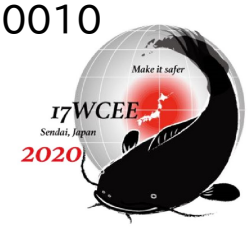

6. Acknowledgements

The authors are grateful for financial supports from the Open Foundation of State Key Laboratory of Disaster Reduction in Civil Engineering, Tongji University in China under Grant SLDRCE19-01; the Foundation of Public Welfare Technology Research Project of Zhejiang Province in China under Grant LGF20E080013; the Foundation of Public Welfare Technology Research Project of Ningbo in China under Grant 2019C50011; the Ningbo Natural Science Foundation in China under Grant 2018A610355.

References

[1] Mwafy Aman, Sayed K (2017): Effect of Vertical Structural Irregularity on Seismic Design of Tall Buildings." *The Structural Design of Tall and Special Buildings,* **26** (18): e1399.

[2] Alavi B, Helmut K (2004): Strengthening of Moment-Resisting Frame Structures against near-Fault Ground Motion Effects. *Earthquake Engineering & Structural Dynamics,* **33** (6): 707–722.

[3] Qu Z, Akira W, Shojiro M, Hiroyasu S, Shoichi K (2012): Pin-Supported Walls for Enhancing the Seismic Performance of Building Structures. *Earthquake Engineering & Structural Dynamics,* **41** (14): 2075–2091.

[4] Khan FR, Sbarounis JA (1993): Interaction of Shear Walls and Frames. *J. Struct. Div., ASCE* **90** (3): 1319 – 1338.

[5] Miranda E (1999): Approximate Seismic Lateral Deformation Demands in Multistory Buildings. *Journal of Structural Engineering,* **125** (4): 417–425.

[6] Pan P, Wu SJ, Nie X (2015): A Distributed Parameter Model of a Frame Pin-Supported Wall Structure. *Earthquake Engineering & Structural Dynamics,* **44** (10): 1643–1659.

[7] Wu SJ, Pan P, Zhang DB (2016): Higher Mode Effects in Frame Pin-Supported Wall Structure. *Earthquake Engineering & Structural Dynamics,* **45** (14): 2371–2387.

[8] Wiebe L, Constantin C (2015): A Cantilever Beam Analogy for Quantifying Higher Mode Effects in Multistorey Buildings. *Earthquake Engineering and Structural Dynamics,* **44** (11): 1697–1716.

[9] Feng YL, Wu J, Chong X, Meng SP (2018): Seismic Lateral Displacement Analysis and Design of an Earthquake-Resilient Dual Wall-Frame System. *Engineering Structures,* **177** (December): 85–102.

[10] Miranda E, Carlos JR (2002): Approximate Lateral Drift Demands in Multistory Buildings with Nonuniform Stiffness. *Journal of Structural Engineering* **128** (7): 840–849.

[11] American Society of Civil Engineers (2010): Minimum Design Loads for Buildings and Other Structures. *ASCE/SEI7-10 Reston,* VA: American Society of Civil Engineers.

[12] Wu DY, Zhao B, Lu XL (2018): Dynamic Behavior of Upgraded Rocking Wall-Moment Frames Using an Extended Coupled-Two-Beam Model. *Soil Dynamics and Earthquake Engineering,* **115** (December): 365–377.

[13] Mazzoni S, Frank M, Michael HS, Gregory LF (2004): OpenSees Users Manual. *PEER,* University of California, Berkeley.

[14] Macrae G, Yoshihiro K, Charles R (2004): Effect of Column Stiffness on Braced Frame Seismic Behavior. *Journal of Structural Engineering-Asce* - J STRUCT ENG-ASCE 130.

[15] Timoshenko SP, Gere JM (1972): Mechanics of Materials. Van Nostrand Reinhold Company.

